Simulation of bluff-body flows through a hybrid RANS/ VMS-LES model

Maria Vittoria SALVETTI[1], Bruno KOOBUS[2], Simone CAMARRI[1], Alain DERVIEUX[3]

[1] *Dipartimento di Ingegneria Aerospaziale, Università di Pisa, Via G. Caruso, 56122 Pisa, Italy.*
[2] *Département de Mathématiques, Université de Montpellier II, Place E. Bataillon, 34095 Montpellier, France.*
[3] *INRIA, 2004 Route des Lucioles, 06902 Sophia-Antipolis, France.*

Abstract. A new strategy is proposed for blending RANS and LES approaches in a hybrid model. To this purpose, the flow variables are decomposed in a RANS part (i.e. the averaged flow field), a correction part that takes into account the turbulent large-scale fluctuations, and a third part made of the unresolved or SGS fluctuations. The basic idea is to solve the RANS equations in the whole computational domain and to correct the obtained averaged flow field by adding, where the grid is adequately refined, the remaining resolved fluctuations. To obtain a model which progressively switches from the RANS to the LES mode, a smooth blending function is introduced to damp the correction term. Different definitions of the blending function are proposed and investigated. The capabilities of the proposed hybrid approach are appraised in the simulation of the flow around a square cylinder at a Reynolds number equal to $Re = 22000$, and in the simulation of the flow around a circular cylinder at $Re = 140000$. Results are compared to those of other hybrid simulations in the literature and to experimental data.

Key words: hybrid RANS/LES approach, bluff-body flows, variational multi-scale LES.

1. Introduction

The most widely used approach for the simulation of high-Reynolds number turbulent flows is the one based on the Reynolds-Averaged Navier-Stokes equations (RANS). However, RANS models usually have difficulties in providing accurate predictions for flows with massive separations, as for instance the flow around bluff bodies. An alternative approach is the Large-Eddy simulation (LES), which, for massively separated flows, is generally more accurate, but also computationally more expensive, than RANS. Moreover, the cost of LES simulations increases as the flow Reynolds number is increased. Indeed, the grid has to be fine enough to resolve a significant part of the turbulent scales, and this becomes particularly critical in the near-wall regions. A new class of models has recently been proposed in the literature in which RANS and LES approaches are combined together in order to obtain simulations as accurate as in the LES case but at reasonable computational costs. Among the hybrid models described in the literature, the Detached Eddy Simulation (DES) has received the largest attention. This approach [21] is generally based on the Spalart-Allmaras RANS model, modified in such a way that, far from solid walls and with refined grids, the simulation switches to the LES mode with a one-equation SGS closure. Another hybrid approach has been recently proposed (LNS, [2]), in

which the blending parameter depends on the values of the eddy-viscosity given by a RANS model and of the SGS viscosity given by a LES closure. In practice, the minimum of the two eddy-viscosities is used. An example of validation of LNS for the simulation of bluff-body flows is given in [5].
A major difficulty in combining a standard RANS model with a LES one is due to the fact that RANS does not naturally allow for fluctuations, due to its tendency to damp them and to "perpetuate itself", as explained in [21]. On the other hand, LES needs a significant level of fluctuations in order to model the flow accurately enough. The abrupt passage from a RANS region to a LES one may produce the so-called "modeled stress depletion" [21]. In the present work, a new strategy is proposed for blending RANS and LES approaches in a hybrid model. To this purpose, as in [12], the flow variables are decomposed in a RANS part (i.e. the averaged flow field), a correction part that takes into account the turbulent large-scale fluctuations, and a third part made of the unresolved or SGS fluctuations. The basic idea is to solve the RANS equations in the whole computational domain and to correct the obtained averaged flow field by adding, where the grid is adequately refined, the remaining resolved fluctuations. We search here for a hybridization strategy in which the RANS and LES models are blended in the computational domain following a given criterion. To this aim, a blending function is introduced, θ, which smoothly varies between 0 and 1. The correction term which is added to the averaged flow field is thus damped by a factor $(1-\theta)$, obtaining a model which coincides with the RANS approach when $\theta = 1$ and recovers the LES approach in the limit of $\theta \to 0$. Following strictly these guidelines would imply that the two fields, RANS and LES correction, need to be computed separately. In this first paper, we explore a single field version and investigate several other ingredients of the proposed hybrid family. In particular, three different definitions of the blending function θ are proposed and will be examined in this paper. They are based on the ratios between (i) two eddy viscosities, (ii) two characteristic length scales and (iii) two characteristic time scales given by the RANS and the LES models, respectively. The RANS model used in the proposed hybrid approach is the standard $k-\varepsilon$ model [13] or a low-Reynolds version [7], while for the LES part the Variational Multi-Scale approach (VMS) is adopted [9]. The proposed hybridization strategy permits a natural integration of the VMS concept, while this is not the case for other existing approaches, as LNS or DES. The VMS approach can be compared in terms of accuracy to the dynamic Smagorinsky model, but its computational cost is definitely lower and comparable to that of the simple Smagorinsky model (see [11]). Extension of VMS to unstructured meshes [11] [19] is a further step to industrial applications.
The capabilities of the proposed hybrid approach are appraised, first, in the simulation of the flow around a square cylinder at a Reynolds number, based on the far-field velocity and on the side length of the cylinder, equal to $Re = 22000$. Different simulations have been carried out by varying the grid refinement and the definition of the blending function. The obtained results are compared with experimental data, the results of LES and DES simulations in the literature, and with those obtained by the same code through the LNS approach. The proposed model is also applied to the simulation of the flow around a circular cylinder at $Re = 140000$ (based on the far-field velocity and the cylinder diameter). Comparisons with experimental data and DES simulations in the literature are provided also for this latter test case.

2. Hybrid RANS/LES coupling

The Navier-Stokes equations for compressible flows of (calorically and thermally) perfect Newtonian gases are considered here, in conservative form and using the following variables: density (ρ), momentum (ρu_i, $i = 1, 2, 3$) and total energy per unit volume ($E = \rho e + 1/2 \rho u_i u_i$, e being the internal energy).
As in [12], the following decomposition of the flow variables is adopted:

$$W = \underbrace{< W >}_{RANS} + \underbrace{W^c}_{correction} + W^{SGS}$$

where $< W >$ are the RANS flow variables, obtained by applying an averaging operator to the Navier-Stokes equations, W^c are the remaining resolved fluctuations (i.e. $< W > + W^c$ are the flow variables in LES) and W^{SGS} are the unresolved or SGS fluctuations.
If we write the Navier-Stokes equations in the following compact conservative form:

$$\frac{\partial W}{\partial t} + \nabla \cdot F(W) = 0$$

in which F represents both the viscous and the convective fluxes, for the averaged flow $\langle W \rangle$ we get:

$$\frac{\partial \langle W \rangle}{\partial t} + \nabla \cdot F(\langle W \rangle) = -\tau^{RANS}(\langle W \rangle) \tag{1}$$

where $\tau^{RANS}(\langle W \rangle)$ is the closure term given by a RANS turbulence model.
As well known, by applying a filtering operator to the Navier-Stokes equations, the LES equations are obtained, which can be written as follows:

$$\frac{\partial \langle W \rangle + W^c}{\partial t} + \nabla \cdot F(\langle W \rangle + W^c) = -\tau^{LES}(\langle W \rangle + W^c) \tag{2}$$

where τ^{LES} is the SGS term.
An equation for the resolved fluctuations W^c can thus be derived (see also [12]):

$$\frac{\partial W^c}{\partial t} + \nabla \cdot F(\langle W \rangle + W^c) \; - \; \nabla \cdot F(\langle W \rangle) = \tau^{RANS}(\langle W \rangle) - \tau^{LES}(\langle W \rangle + W^c) \tag{3}$$

The basic idea of the proposed hybrid model is to solve Eq. (1) in the whole domain and to correct the obtained averaged flow by adding the remaining resolved fluctuations (computed through Eq. (3)), wherever the grid resolution is adequate for a LES. To identify the regions where the additional fluctuations must be computed, we introduce a *blending function*, θ, smoothly varying between 0 and 1. When $\theta = 1$, no correction to $\langle W \rangle$ is computed and, thus, the RANS approach is recovered. Conversely, wherever $\theta < 1$, additional resolved fluctuations are computed; in the limit of $\theta \to 0$ we want to recover a full LES approach. Thus, the following equation is used here for the correction term:

$$\frac{\partial W^c}{\partial t} + \nabla \cdot F(\langle W \rangle + W^c) - \nabla \cdot F(\langle W \rangle) = (1-\theta) \left[\tau^{RANS}(\langle W \rangle) - \tau^{LES}(\langle W \rangle + W^c)\right] \tag{4}$$

Note that for $\theta \to 1$ the RANS limit is actually recovered; indeed, for $\theta = 1$ the right-hand side of Eq. (4) vanishes and, hence, a trivial solution is $W^c = 0$. As required, for $\theta = 0$ Eq. (4) becomes identical to Eq. (3) and the remaining resolved fluctuations are added to the averaged flow; the model, thus, works in LES mode. For θ going from 1 to 0, i.e. when, following the definition of the blending function (see Sec. 5.), the grid resolution is intermediate between one adequate for RANS and one adequate for LES, the righthandside term in Eq. (4) is damped through multiplication by $(1 - \theta)$. Although it could seem rather arbitrary from a physical point of view, this is aimed to obtain a smooth transition between RANS and LES. More specifically, we wish to obtain a progressive addition of fluctuations when the grid resolution increases and the model switches from the RANS to the LES mode. Summarizing, the ingredients of the proposed approach are: a RANS closure model, a SGS model for LES and the definition of the blending function. These will be described in Secs. 4 and 5.

3. Basic numerical ingredients

The governing equations are discretized in space using a mixed finite-volume/finite-element method applied to unstructured tetrahedrizations. The adopted scheme is vertex centered, i.e. all degrees of freedom are located at the vertexes. P1 Galerkin finite elements are used to discretize the diffusive terms. A dual finite-volume grid is obtained by building a cell C_i around each vertex i. The convective fluxes are discretized in terms of fluxes through the common boundaries shared by neighboring cells. The Roe scheme [16] represents the basic upwind component for the numerical evaluation of the convective fluxes. A Turkel-type preconditioning term is introduced to avoid accuracy problems at low Mach numbers [8]. A parameter γ_s multiplies the upwind part of the scheme and permits a direct control of the numerical viscosity, leading to a full upwind scheme for $\gamma_s = 1$ and to a centered scheme when $\gamma_s = 0$. The MUSCL linear reconstruction method ("Monotone Upwind Schemes for Conservation Laws" [23]) is employed to increase the order of accuracy of the Roe scheme. A reconstruction using a combination of different families of approximate gradients is adopted [4], which allows a numerical dissipation made of sixth-order space derivatives, and, thus, concentrated on a narrow-band of the highest resolved frequencies, to be obtained. This is important in LES simulations to limit as far as possible the interactions between numerical and SGS dissipation, which could deteriorate the accuracy of the results.
An implicit time marching algorithm is used, based on a second-order time-accurate backward difference scheme.
More details on the numerical ingredients used in the present work can be found in [4] and [6].

4. RANS and VMS-LES closures

As far the closure of the RANS equations is concerned, the standard $k-\varepsilon$ model [13] is used, in which the Reynolds stress tensor is modeled by introducing a turbulent eddy-viscosity μ_t, defined as a function of the turbulent kinetic energy k and of the turbulent dissipation rate of energy, ε, as follows:

$$\mu_t = C_\mu \rho \frac{k^2}{\varepsilon} \tag{5}$$

where C_μ is a model parameter, set here equal to the classical value of 0.09 and k and ε are obtained from the corresponding modeled transport equations (see Ref. [13]). The Low Reynolds $k-\varepsilon$ model proposed in [7] is also considered. The Reynolds stress tensor has the same form of that used in the standard $k-\varepsilon$ model but here the turbulent eddy-viscosity μ_t given by Eq. (5) is multiplied by a damping function f_μ, and k and ε are determined by ad-hoc modeled transport equations (see [7]).
For the LES mode, we wish to recover the Variational Multi-Scale approach [9], in which the flow variables are decomposed as follows:

$$W = \underbrace{\overline{W}}_{LRS} + \underbrace{W'}_{SRS} + W^{SGS} \tag{6}$$

where $\overline{W}$ are the large resolved scales (LRS) and W' are the small resolved scales (SRS). This decomposition is obtained by variational projection in the LRS and SRS spaces respectively. In the present study, we follow the VMS approach proposed in [11] for the simulation of compressible turbulent flows through a finite volume/finite element discretization on unstructured tetrahedral grids. Let χ_l and ϕ_l be the N finite-volume and finite-element basis functions associated to the used grid. In order to obtain the VMS flow decomposition, the finite dimensional spaces $\mathcal{V}_{FV}$ and $\mathcal{V}_{FE}$, respectively spanned by χ_l and ϕ_l, can be in turn decomposed in $\overline{\mathcal{V}}_{FV}$ and $\mathcal{V}'_{FV}$ and in $\overline{\mathcal{V}}_{FE}$ and $\mathcal{V}'_{FE}$ [11], $\overline{\mathcal{V}}_{FV}$ and $\mathcal{V}'_{FV}$ being the finite volume spaces associated to the largest and smallest resolved scales, spanned by the basis functions $\overline{\chi_l}$ and χ'_l; $\overline{\mathcal{V}}_{FE}$ and $\mathcal{V}'_{FE}$ are the finite element analogous. In [11] a projector operator P in the LRS space is defined by spatial average on macro cells, obtained by agglomeration.
Finally, a key feature of the VMS approach is that the SGS model is added only to the smallest resolved scales. As in [11], the Smagorinsky model is used, and, hence, the SGS terms are discretized analogously to the viscous fluxes. Thus, the Galerkin projection of Eq. (2) becomes:

$$\begin{aligned}&\left(\frac{\partial \langle W\rangle + W^c}{\partial t}, \chi_l\right) + (\nabla\cdot F_c(\langle W\rangle + W^c), \chi_l) + \\ &(\nabla\cdot F_v(\langle W\rangle + W^c), \phi_l) = -\left(\ \tau^{LES}(W'), \phi'_l\right) \quad l=1,N\end{aligned} \tag{7}$$

in which τ_{LES} is modeled by introducing a SGS eddy-viscosity μ_s, having the following expression:

$$\mu_s = \rho' C_s \Delta^2 \sqrt{S'_{ij}S'_{ij}} \tag{8}$$

where C_s is the model input parameter, S'_{ij} is the strain-rate tensor (computed in the VMS approach as a function of W') and Δ is a length which should be representative of the size of the resolved turbulent scales. Here, Δ has been selected as $Vol(i)^{1/3}$ ($Vol(i)$ being the volume of the i-th tetrahedron) and C_s has been set equal to 0.1.
Finally, the Galerkin projection of Eqs. (1) and (4) for the computation of $\langle W\rangle$ and of the additional fluctuations in the proposed hybrid model become respectively:

$$\begin{aligned}&\left(\frac{\partial \langle W\rangle}{\partial t}, \chi_l\right) + (\nabla\cdot F_c(\langle W\rangle), \chi_l) + (\nabla\cdot F_v(\langle W\rangle), \phi_l) = \\ &-\left(\tau^{RANS}(\langle W\rangle), \phi_l\right) \quad l=1,N\end{aligned} \tag{9}$$

$$\begin{aligned}&\left(\frac{\partial W^c}{\partial t}, \chi_l\right) + (\nabla\cdot F_c(\langle W\rangle + W^c), \chi_l) - (\nabla\cdot F_c(\langle W\rangle), \chi_l) + \\ &(\nabla\cdot F_v(W^c), \phi_l) = (1-\theta)\left[\left(\ \tau^{RANS}(\langle W\rangle), \phi_l\right) - \left(\tau^{LES}(W'), \phi'_l\right)\right] \quad l=1,N\end{aligned} \tag{10}$$

5. Definition of the blending function and simplified model

As a possible choice for θ, the following function is used in the present study:

$$\theta = F(\xi) = tanh(\xi^2) \tag{11}$$

where ξ is the *blending parameter*, which should indicate whether the grid resolution is fine enough to resolve a significant part of the turbulence fluctuations, i.e. to obtain a LES-like simulation. The choice of the *blending parameter* is clearly a key point for the definition of the present hybrid model. In the present study, different options are proposed and investigated, namely: the ratio between the eddy viscosities given by the LES and the RANS closures, $\xi_{VR} = \mu_s/\mu_t$, which is also used as a blending parameter in LNS Ref. [2], $\xi_{LR} = \Delta/l_{RANS}$, l_{RANS} being a typical length in the RANS approach, i.e. $l_{RANS} = k^{3/2}\epsilon^{-1}$ and, finally, $\xi_{TR} = t_{LES}/t_{RANS}$, t_{LES} and t_{RANS} being characteristic times of the LES and RANS approaches respectively, $t_{LES} = (S_{ij}S_{ij})^{-1/2}$ and $t_{RANS} = k\epsilon^{-1}$.
To avoid the solution of two different systems of PDEs and the consequent increase of required computational resources, Eqs. (9) and (10) can be recast together as:

$$\begin{aligned}&\left(\frac{\partial W}{\partial t}, \chi_l\right) + (\nabla \cdot F_c(W), \chi_l) + (\nabla \cdot F_v(W), \phi_l) = \\ &-\theta \left(\tau^{RANS}(\langle W \rangle), \phi_l\right) - (1-\theta)\left(\tau^{LES}(W'), \phi_l'\right) \quad l = 1, N\end{aligned} \tag{12}$$

Clearly, if only Eq. (12) is solved, $\langle W \rangle$ is not available at each time step. Two different options are possible: either to use an approximation of $\langle W \rangle$ obtained by averaging and smoothing of W, in the spirit of VMS, or to simply use in Eq. (12) $\tau^{RANS}(W)$. The second option is adopted here as a first approximation.

6. Hybrid simulations of the flow around a square cylinder

The flow around a square cylinder is considered at a Reynolds number, based on the cylinder side length, D, and on the free-stream velocity, is equal to 22000. The dimensions of the computational domain are reported in Tab. 1. They are equal to those employed in the LNS simulation in [5]. Two different unstructured grids made of tetrahedral elements (grid GR1 and GR2 in Tab. 1) are used for the simulations. Note that both grids are significantly coarser than those typically used in the literature for LES, but also for DES simulations, of this flow. We chose to use coarse grids in order to have the model working in hybrid mode, since both the LNS and the proposed approach tend to LES if the grid is adequately refined (see [5]). Approximate boundary conditions, based on the Reichardt wall-law, are applied at the solid walls. This type of wall treatment has been successfully used in previous LES (see e.g. [4], [11]) and LNS [5] simulations of the same flow. At the inflow, the flow is assumed to be undisturbed and radiative boundary conditions are used at the outflow (see [5]). On the other surfaces ($y = \pm H_y$, $z = \pm H_z$) slip conditions are imposed. Following the LNS work in Ref. [5], the numerical parameter γ_s, which controls the amount of numerical viscosity introduced in the simulation, has been set equal to 0.1 for GR1 and 0.5 for GR2, in order to obtain stable simulations.
The simulations have been implicitly advanced in time, with a maximum CFL number ranging from 10 to 20. In a previous work (Ref. [5]), it was shown that no significant information is lost in time provided that CFL$\leq$ 25.

	l_i/D	l_o/D	H_y/D	H_z/D	N. nodes	N. elements
Gr1	4.5	9.5	7	9.75	8.3×10^4	4.75×10^5
Gr2	4.5	9.5	7	9.75	3.5×10^4	1.9×10^5

Table 1. Main features of the computational domain and grids for the square cylinder test case. l_i is the streamwise distance between the inflow and the cylinder center. l_o is the streamwise distance between the outflow and the cylinder center. H_y and H_z are the lateral and spanwise dimensions of the domain.

Simulations	Grid	Model	ξ	$\overline{C_d}$	C'_d	C'_l	St	l_r
LNS1	Gr1	LNS	–	2.11	0.116	0.654	0.131	1.15
LNS2	Gr2	LNS	–	2.07	0.087	0.685	0.13	1.19
CHM1	Gr1	CHM	VR	1.95	0.107	0.81	0.13	1.37
CHM2	Gr1	CHM	TR	2.01	0.117	0.792	0.131	1.16
CHM3	Gr2	CHM	VR	2.01	0.074	0.58	0.129	1.1
CHM4	Gr2	CHM	TR	2.01	0.071	0.6	0.131	1.21
CHM5	Gr2	CHM	LR	2.01	0.083	0.63	0.128	1.1
LES [5]	Gr2	[20]	–	1.71	0.02	0.31	0.137	2.8
RANS [5]	Gr2	$k-\varepsilon$	–	1.53	0.01	0.20	0.117	2.38
DES [18]	–	DES	–	2.42-2.57	0.28-0.68	1.36-1.55	0.09-0.13	1.16-1.37
DES [14]	–	DES	–	2.18	–	–	0.134	0.81
Exp. [3]	–	–	–	2.28	–	1.2	0.13	–
Exp. [15]	–	–	–	2.1	–	–	0.132	1.4

Table 2. Simulation parameters and main bulk flow quantities for the square cylinder test case.

For both grids, the computations have been carried out using the LNS model and the new proposed hybrid model (*Continuous Hybrid Model*, CHM) with different definitions of the blending parameter. The parameters characterizing the different simulations are summarized in Tab. 2. Tab. 2 also shows the main bulk flow parameters, viz. the mean drag coefficient $\overline{C_d}$, the r.m.s. values of the drag and lift coefficients, C'_d and C'_l, the vortex shedding frequency adimensionalized with D and the free-stream velocity, St, and the mean recirculation bubble length, l_r. Let us analyze, first, the sensitivity to grid refinement by comparing CHM1 with CHM3 and CHM2 with CHM4. The most significant differences are in the force r.m.s., and, in particular, larger fluctuations are found for the more refined grid. This is consistent with the basic idea of the proposed model, i.e. to progressively add more fluctuations as the grid resolution increases. As for the definition of the blending parameter, its effect on the computed flow bulk parameters is rather small, the most sensitive quantity being l_r with a variation of 15% between CHM1 and CHM2. The overall agreement with the experimental values is fairly good, especially reminding the very coarse grid resolution of the present simulations. Note that, as reported in Tab. 2, LES and RANS simulations carried out on the same grid give inaccurate predictions. As previously mentioned, the results of DES reported in Tab. 2 are obtained with significantly finer grid resolution.

Finally, the behavior of the proposed hybrid model in the field (not shown here for

Simulations	Re	ξ	$\overline{C_d}$	C_l'	St	l_r	θ_{sep}
CHM1	$1.4\ 10^5$	VR	0.62	0.083	0.30	1.20	108
CHM2	$1.4\ 10^5$	LR	0.62	0.083	0.30	1.19	108
DES [22]	$1.4\ 10^5$	–	0.57-0.65	0.08-0.1	0.28-0.31	1.1 -1.4	93-99
DES [14]	$1.4\ 10^5$	–	0.6-0.81	–	0.29-0.3	0.6-0.81	101-105
Exp. [10]	$3.8\ 10^6$	–	0.58	–	0.25	–	110
Exp. [1]	$5\ 10^6$	–	0.7	–	–	–	112
Exp. [17]	$8\ 10^6$	–	0.52	0.06	0.28	–	–

Table 3. Simulation parameters and main bulk flow quantities for the circular cylinder test case. Same notations as in Tab. 2. θ_{sep} is the separation angle.

the sake of brevity) is very similar for all the considered definitions of the blending parameter and grids. In particular, the model works in the LES mode in the wake, in the RANS mode in the shear-layers detaching from the cylinder corners, while damped fluctuations are added in a layer at the wake edges.

7. Hybrid simulations of the flow around a circular cylinder

The proposed approach has also been applied to the simulation of the flow around a circular cylinder at $Re = 140000$ (based on the far-field velocity and the cylinder diameter). The domain dimensions are $l_i/D = 5$, $l_o/D = 15$, $H_y/D = 7$ and $H_z/D = 2$ (the symbols are the same as in Tab. 1). The used grid has 4.6×10^5 nodes. The inflow conditions are the same as in the DES simulations of [22]. In particular, the flow is assumed to be highly turbulent by setting the inflow value of eddy-viscosity to about 5 times the molecular viscosity as in the DES simulation of [22]. This setting corresponds to a free-stream turbulence level $Tu = \overline{u'^2}/U_0$ (where u' is the inlet fluctuation velocity and U_0 is the free-stream mean velocity) of the order of 4%. As discussed also in [22], the effect of such a high level of free-stream turbulence is to make the boundary layer almost entirely turbulent also at the relatively moderate considered Reynolds number. The boundary treatment is the same as for the square cylinder test-case, except that the flow is assumed to be periodic in the spanwise direction in order to simulate a cylinder of infinite spanwise length. The computations have been carried out using the new proposed hybrid model with two different definition of the blending parameter(see Tab. 3). The RANS model is that based on the *Low Reynolds* approach discussed in Sec. 4. The numerical parameter γ_s, which controls the amount of numerical viscosity introduced in the simulation, has been set equal to 0.2.
The main flow bulk parameters obtained in the present simulations are summarized in Tab. 3, together with the results of DES simulations in the literature and some experimental data. The results are also for this case practically insensitive to the definition of the blending parameter. The agreement with the DES results is fairly good. As for the comparison with the experiments, as also stated in [22], since our simulations are characterized by a high level of turbulence intensity at the inflow, it make sense to compare the results with experiments at higher Reynolds number, in which, although the level of turbulence intensity of the incoming flow is very low, the transition to turbulence of the boundary layer occurs upstream separation. The

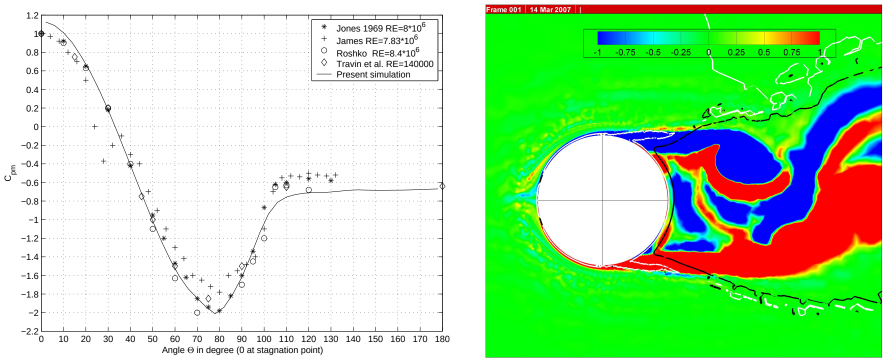

Figure 1. (a) Mean pressure coefficient on the cylinder (simulation CHM1) (b) Instantaneous isocontours of spanwise vorticity (simulation CHM2). The black and white lines are the isolines of $\theta = 0.1$ and $\theta = 0.9$.

agreement with these high *Re* experiments is indeed fairly good, as shown in Tab. 3 and Fig. 1a. Finally, the behavior of the hybridization strategy in the field is similar to that obtained for the square cylinder test case; indeed, as shown in Fig. 1b, the model works in RANS mode in the boundary layer and in the shear-layers detaching from the cylinder, while in the wake a full LES correction is recovered.

8. Concluding remarks

A new strategy for blending RANS and LES has been proposed, which is based on a decomposition of the flow variables in a RANS part and a correction part, which takes into account the resolved fluctuations. To identify the zones in which the correction must be computed and added to the RANS part, a blending function is introduced, such that the model works in RANS mode where the grid is coarse and tends with continuity to LES as the grid refinement becomes adequate. For the closure of the LES part, the VMS approach has been integrated in the proposed hybridization strategy. As a first choice, we use here a simplified version of the model, in which only one set of unknowns is computed. The proposed method has been applied to the hybrid simulations of the flows around two different bluff-bodies, viz. a square cylinder and a circular one. The results are promising, both for the accuracy of the prediction of the bulk flow parameters, which is in good agreement with experimental data and the results of different simulations in the literature, and for the behavior of the blending function, which shows a sensible distribution in the field.

References

[1] E. Achenbach. Distribution of local pressure and skin friction around a circular cylinder in cross-flow up to Re= 5×10^6. *J. Fluid Mech.*, 34(4):625–639, 1968.

[2] P. Batten, U. Goldberg, and S. Chakravarthy. Interfacing statistical turbulence closures with large-eddy simulation. *AIAA Journal*, 42(3):485–492, 2004.

[3] P.W. Bearman and E.D. Obasaju. An experimental study of pressure fluctuations on fixed and oscillating square-section cylinders. *J. Fluid Mech.*, 119:297–321, 1982.

[4] S. Camarri, M. V. Salvetti, B. Koobus, and A. Dervieux. A low diffusion MUSCL scheme for LES on unstructured grids. *Computers and Fluids*, 33:1101–1129, 2004.

[5] S. Camarri, M.V. Salvetti, B. Koobus, and A. Dervieux. Hybrid RANS/LES simulations of a bluff-body flow. *Wind & Structures*, 8:407–426, 2005.

[6] C. Farhat, B. Koobus, and H. Tran. Simulation of vortex shedding dominated flows past rigid and flexible structures. In *Computational Methods for Fluid-Structure Interaction*, pages 1–30. Tapir, 1999.

[7] U. Goldberg, O. Peroomian, and S. Chakravarthy. A wall-distance-free $k - \varepsilon$ model with enhanced near-wall treatment. *Journal of Fluids Engineering*, 120:457–462, 1998.

[8] H. Guillard and C. Viozat. On the behaviour of upwind schemes in the low Mach number limit. *Computers and Fluids*, 28:63–86, 1999.

[9] T.J.R. Hughes, L. Mazzei, and K.E. Jansen. Large eddy simulation and the variational multiscale method. *Comput. Vis. Sci.*, 3:47–59, 2000.

[10] W.D. James, S.W. Paris, and G.V. Malcolm. Study of viscous cross flow effects on circular cylinders at high Reynolds numbers. *AIAA Journal*, 18:1066–1072, 1980.

[11] B. Koobus and C. Farhat. A variational multiscale method for the large eddy simulation of compressible turbulent flows on unstructured meshes-application to vortex shedding. *Comput. Methods Appl. Mech. Eng.*, 193:1367–1383, 2004.

[12] E. Labourasse and P. Sagaut. Reconstruction of turbulent fluctuations using a hybrid RANS/LES approach. *J. Comp. Phys.*, 182:301–336, 2002.

[13] B.E. Launder and D.B. Spalding. The numerical computation of turbulent flows. *Comp. Meth. Appl. Mech. and Eng.*, 3:269–289, 1979.

[14] S.-C. Lo, K.A. Hofmann, and J.-F. Dietiker. Numerical investigation of high Reynolds number flows over square and circular cylinder. *Journal of Thermophysics and Heat Transfer*, 19:72–80, 2005.

[15] D.A. Lyn and W. Rodi. The flapping shear layer formed by flow separation from the forward corner of a square cylinder. *J. Fluid Mech.*, 267:353–376, 1994.

[16] P.L. Roe. Approximate Riemann solvers, parameters, vectors and difference schemes. *J. Comp. Phys.*, 43:357–372, 1981.

[17] J.W. Schewe. On the forces acting on a circular cylinder in cross flow from subcritical up to transcritical Reynolds numbers. *J. Fluid Mech.*, 133:265–285, 1983.

[18] S. Schmidt and F. Thiele. Comparison of numerical methods applied to the flow over wall-mounted cubes. *Int. J. of Heat and Fluid Flow*, 23:330–339, 2002.

[19] S. Sirnivas, S. Wornom, A. Dervieux, B. Koobus, and O. Allain. A study of LES models for the simulation of a turbulent flow around a truss spar geometry. In *Proceedings of OMAE'06, 25rd International Conference on Offshore and Arctic Engineering*, number OMAE2006-92355, Hamburg, Germany, 2006.

[20] J. Smagorinsky. General circulation experiments with the primitive equations. *Monthly Weather Review*, 91(3):99–164, 1963.

[21] P.R. Spalart, W.H. Jou, M. Strelets, and S. Allmaras. *Advances in* DNS/LES, chapter Comments on the feasibility of LES for wings and on a hybrid RANS/LES approach. Columbus (OH), 1997.

[22] A. Travin, M. Shur, M. Strelets, and P. Spalart. Detached-eddy simulations past a circular cylinder. *Flow, Turbulence and Combustion*, 63:293–313, 1999.

[23] B. van Leer. Towards the ultimate conservative scheme. IV: A new approach to numerical convection. *J. Comp. Phys.*, 23:276–299, 1977.